**Supporting Information**

# Synaptic Characteristics of Amorphous Boron Nitride–based Memristors on a Highly Doped Silicon Substrate for Neuromorphic Engineering

*Jinju Lee[1#], Ji-Ho Ryu[1#], Boram Kim[2], Fayyaz Hussain[3], Chandreswar Mahata[1], Eunjin Sim[1], Muhammad Ismail[1], Yawar Abbas[4], Haider Abbas[5], Dong Keun Lee[6], Min-Hwi Kim[6], Yoon Kim[2], Changhwan Choi[5], Byung-Gook Park[6], Sungjun Kim[1]**

[1]School of Electronics Engineering, Chungbuk National University, Cheongju 28644, South Korea

[2]School of Electrical and Computer Engineering, University of Seoul, Seoul, 02504, South Korea

[3]Materials Research Simulation Laboratory (MSRL) Department of physics, Bahauddin Zakariya University Multan, Pakistan

[4]Department of Physics, Khalifa University, Abu Dhabi 127788, United Arab Emirates

[5]Division of Materials Science and Engineering, Hanyang University, Seoul 04763, South Korea

[6]Inter-university Semiconductor Research Center (ISRC) and the Department of Electrical and Computer Engineering, Seoul National University, Seoul 08826, South Korea

*E-mail: sungjun@dongguk.edu

[#]Equally contributed

**Contents:**



To monitor the chemical structure of the a-BN film on Si X-ray photo-electron spectra has been carried out. Fig. S1 shows the XPS spectra for B1s and N1s core level was analyzed with Shirley background and Gaussian-Lorentzian function. High resolution B1s spectrum was fitted with three peaks at 190.8 eV, 192.1 eV and 193.2 eV which are corresponding to the

bonds B–C, B–N, and B–O. The B–C bonding arise from the surface carbon contamination during deposition which at lower binding energy compared to B–N. On the other hand, B–O bonds appear due to the oxidation of the B atoms and it comes at higher binding energy.[1] The N1s spectrum consist of four component situated at 397.3 eV, 398.3 eV, 399.75 eV, and 401.45 eV which are appeared due to the chemical bonding of N-O, N-B, N-C and N-N correspondingly.[2,3]

Figure S2(a) shows I-V characteristics of Pt/BN/Si device. The bipolar switching with only few cycles is observed. The intrinsic switching may be dominant for Pt/BN/Si device because Pt is inert metal. This result supports poor switching of Ti/BN/Si device under negative SET and positive RESET. Figure S2(b) shows the I-V of Cu/BN/Si device. There is no switching for all cells probably due to high diffusivity of Cu ion. Figure S2(c) shows the I-V of Ni/BN/Si device where many switching cycles are observed in one cell but the variation of LRS and HRS are large and switching is not controllable. In Ti/BN/Si device, reset failure occurs in two ways. Figure S3(a) shows no reset switching at a positive bias after set process. It is probably due to the high current from conducting path consisting of boron vacancies. The current overshoot is well known reset failure.[4] Figure S3(b) shows the breakdown after reset process is done. The resistance status is set-stuck and no switching after the breakdown. This is also called negative-set behavior. (This is not set process at a negative bias).[5] Figure S4 shows the temperature dependence of Ti/BN/Si device in the LRS at positive SET and negative RESET with high CC. The resistance increases with temperature indicating that metallic behavior can be explained by Ti diffusion. Figure S5 shows the retention properties in the HRS and LRS at high temperature (85 ˚C) at positive SET and negative RESET with high CC. It can be found that HRS resistance decreases with time. Fig. S6 shows paired-pulse facilitation (PPF) in our artificial synaptic device (Ti/BN/Si device). In biological synapse, PPF refers to a phenomenon

in which a larger synaptic current is detected in the second stimulus when two pairs of stimuli are applied. Here PPF is defined as following:

$$\mathrm{PPF} = \left(\frac{I_{2nd} - I_{1st}}{I_{1st}}\right) \times 100\%$$

where $I_{1st}$ and $I_{2nd}$ are the current of first pulse and second pulse, respectively. It is observed that the current increases in the second pulse, but no clear decay is observed during the interval time. This is probably because this device has good retention.

The methods of neural network simulation are as follows in detail in Fig. S7. We simulated a pattern recognition test with a single layer neural network including input and output neurons. To classify image patterns, Modified National Institute of Standards and Technology (MNIST) dataset is used, which corresponds input neurons. Single layer neuromorphic circuit consists of word lines ($WL_i$, i = 1 ~ 784) for 784 input neurons and bit lines ($BL_j$, j = 0 ~ 9) for 10 output neurons. The memristor array can connect the input and output layers and the conductance of the device corresponds to the weight of the synapse. However, the conductance of a single memristor device alone cannot produce the negative weight value of a synaptic device in real neural networks. Two memristor device pair are used where one synaptic device to express the negative value of the weight. Each synaptic device consists of an exhibitory device and an inhibitory device that plays a role as the exhibitory weight $G^+$ and the inhibitory weight $G^-$, respectively. The weight of the synaptic device is defined as $W_{ij} = G^+ – G^-$. The inference scheme of this system is as follows: The feature of the binary MNIST image (white pixel) is 1 V pulse voltage, and the background (black pixel) is 0 V pulse voltage and applied to the crossbar array through $WL_i$. The input pulse voltage is applied to the exhibitory and inhibitory devices connected to $BL_j^+$ and $BL_j^-$, respectively, and the output voltage can be obtained by multiplying the conductance of the input voltage and the device according to Ohm's law. According to Kirchhoff's current law (KCL), the output currents of devices connected to

$BL_j^+$ are summated to deliver $I_j^+$ and $BL_j^-$ to the output neuron. Finally, the output current ($I_j$) at the output neuron is output as $I_j = I_j^+ – I_j^-$. The label of the output neuron that has the highest value among the $I_j$ output from each of the 10 output neurons ($O_j$, j = 0~ 9) becomes the inference answer.

Learning does not proceed by comparing the inference answer with the true label of the input image. If the answer is not correct, the learning output is increased by increasing the weight of the synaptic devices connected to the output neuron ($O_{TRUE}$) corresponding to the true label so that output current has a value below the exhibit output value (positive value). On the other hand, synaptic devices connected to the output neuron ($O_{FALSE}$), which are not the correct answer, learn to reduce weight so that output current has a value below the inhibit output value (negative value). If the output current of the $O_{TRUE}$ has a value greater than the exhibit output value, the synaptic devices connected to the $O_{TRUE}$ do not update the weight. Likewise, if the output current of $O_{FALSE}$ has a value less than the inhibit output value (negative value), then the synaptic devices connected to the $O_{FALSE}$ will not proceed with the weight update. The increase in $W_{ij}$ is obtained by applying LTP pulse voltage to $G_{ij}^+$ of the device and LTD pulse voltage to $G_{ij}^-$. On the contrary, weight decrease applies the LTP pulse voltage to $G_{ij}^-$ and LTD pulse voltage to $G_{ij}^+$. At this time, the degree of change in weight is determined by the absolute value of the difference between the target output value of each output neuron and the $I_{OUTPUT}$. The greater the difference is, the more the pulse voltage is applied, which increases the degree of change in conductance. On the contrary, as the difference is smaller, the number of pulse voltages is applied to decrease the weight change. All the simulations train 60000 training images in a single-layer neuromorphic system and save the weight map for every 100 training images. The test was conducted by inputting 10000 test images into the stored weight map, and the number of correct images among 10000 test images was expressed as a recognition accuracy as a percentage.

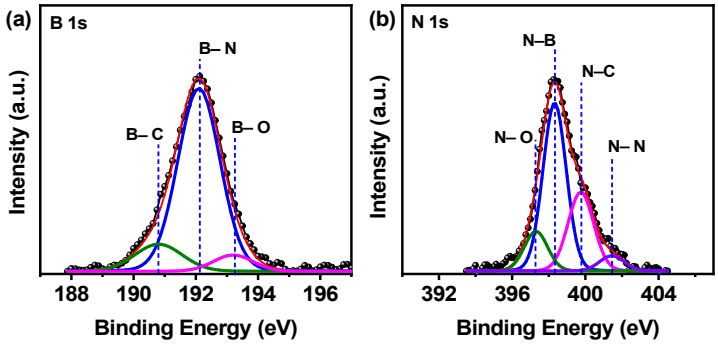


**Figure S1** Deconvoluted XPS spectra of (a) B1s and (b) N1s.

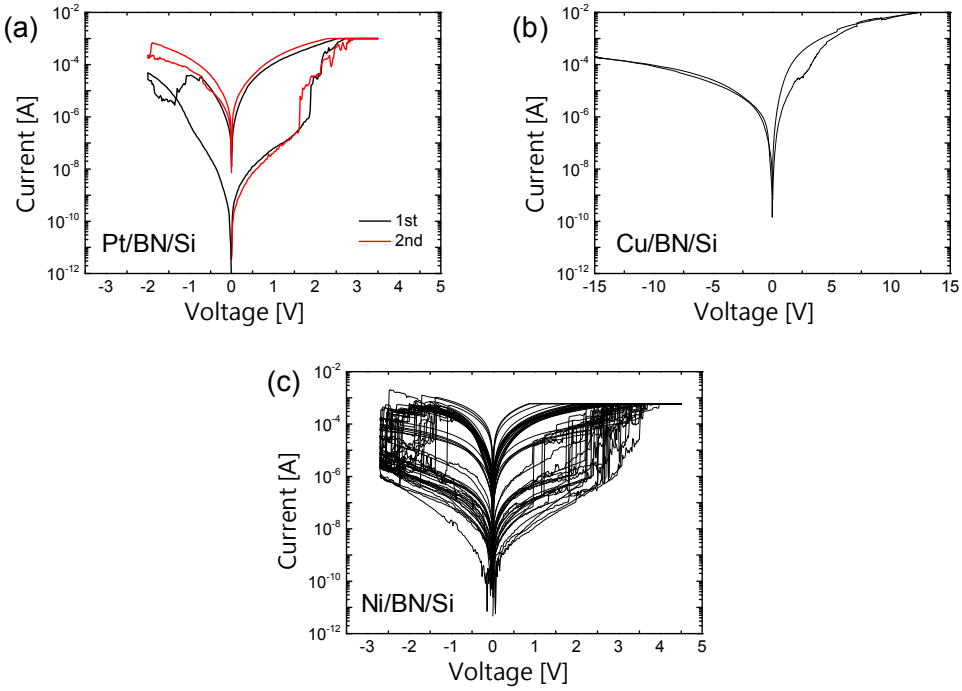


**Figure S2** I-V characteristics of BN/Si device for (a) Pt, (b) Cu, and (c) Ni electrodes.

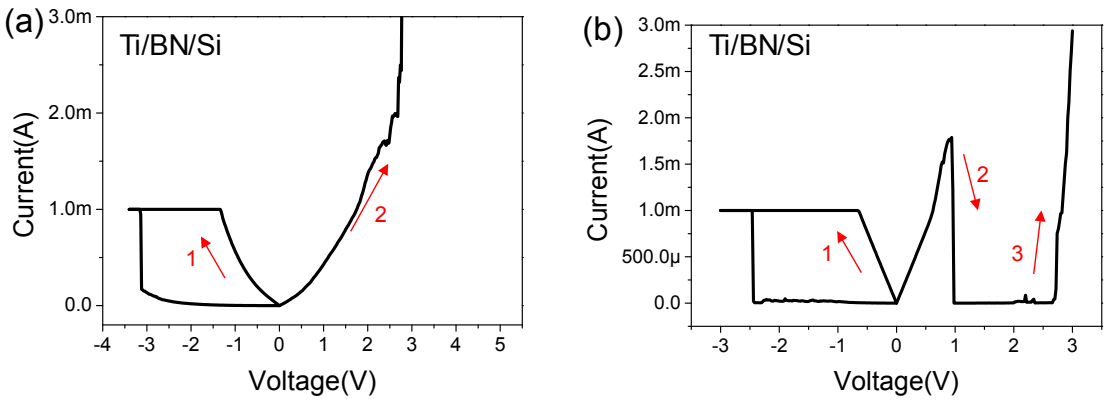


**Figure S3** Reset failure characteristics of Ti/BN/Si device by (a) current overshoot and (b) breakdown after reset event.

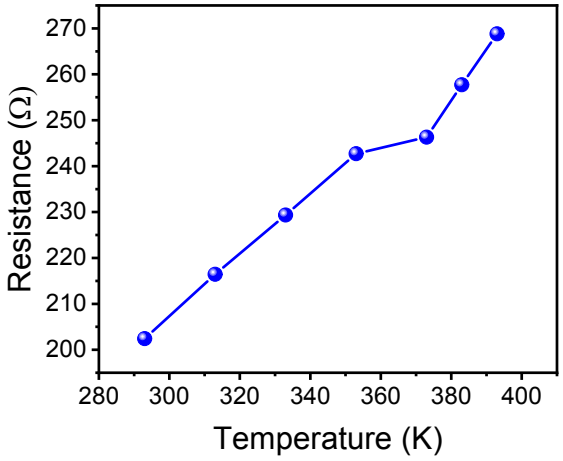


**Figure S4** Temperature dependence of Ti/BN/Si device in the LRS after positive SET.

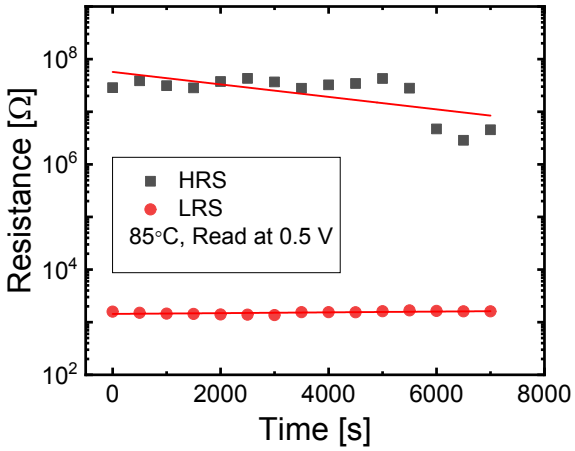


**Figure S5** Retention of Ti/BN/Si device at 85˚C.

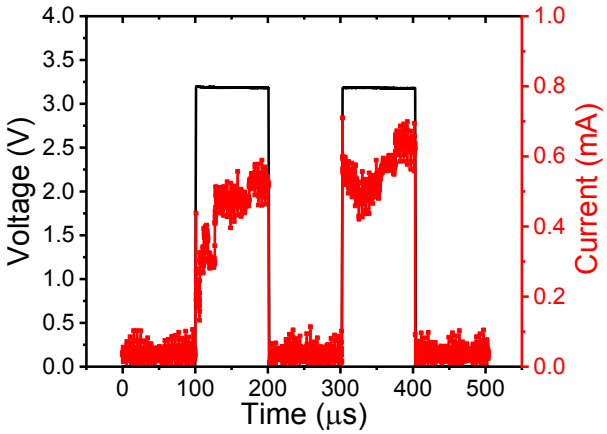


**Figure S6** Paired-pulse facilitation of Ti/BN/Si device.

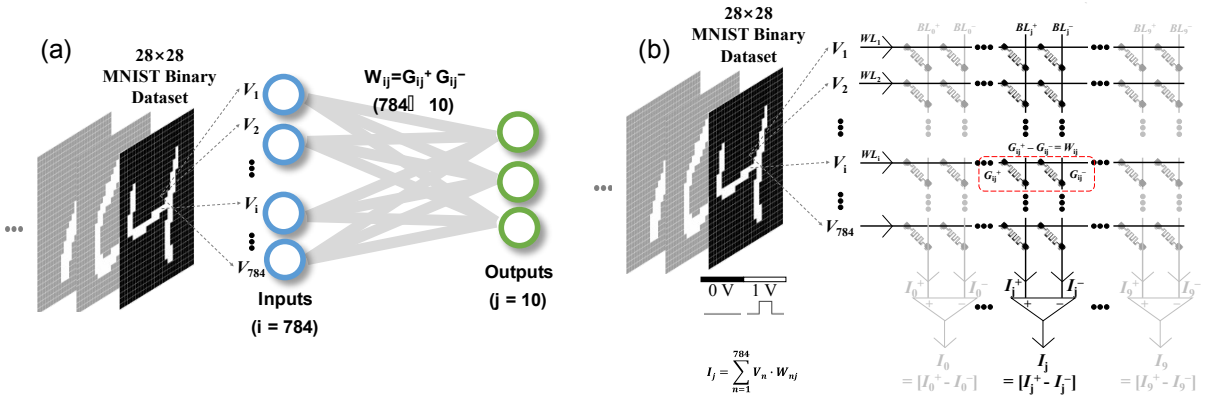


**Figure S7** Neural network simulation configuration for MNIST pattern classification. (a) Single-layer neural network (b) memristor crossbar array implementation of the single-layer neural network.

(1) Pakdel, A.; Wang, W.; Zhi, Z.; Bando, Y.; Watanabe, K.; Sekiguchi, T.; Nakayamaab, T.; Golberg, D. Facile Synthesis of Vertically Aligned Hexagonal Boron Nitride Nanosheets Hybridized with Graphitic Domains, *J. Mater. Chem.*, **2012**, 22, 4818-4824.

(2) Jalaly, M.; Gotor, F. J.; Semnan, M.; Sayagués, M. J.; A Novel, Simple and Rapid Route to the Synthesis of Boron Cabonitride Nanosheets: Combustive Gaseous Unfolding, *Sci. Rep.*, **2017**, 7, 3453.

(3) Xue, Y.; Yu, D.; Dai, L.; Wang, R.; Li, D.; Roy, A.; Lu, F.; Chen, H.; Liu, Y.; Qu, J. Three-Dimensional B, N-Doped Graphene Foam as a Metal-Free Catalyst for Oxygen Reduction Reaction, *Phys. Chem. Chem.* Phys., **2013**, 15, 12220-12226.

(4) Chen, A. Current Overshoot during Set and Reset Operations of Resistive Switching Memories, *IEEE International Reliability Physics Symposium (IRPS)*, **2012**, DOI: 10.1109/IRPS.2012.6241919.

(5) Liu, S.; Zhao, X.; Li, Q.; Li, N.; Wang, W.; Liu, Q.; Xu, H. Analysis of the Negative-SET Behaviors in Cu/$ZrO_2$/Pt Devices, *Nanoscale Res Lett.* **2016,** 11, 542.